

Advancing MAPF towards the Real World: A Scalable Multi-Agent Realistic Testbed (SMART)

Jingtian Yan¹, Zhifei Li¹, William Kang¹, Kevin Zheng², Yulun Zhang¹, Zhe Chen², Yue Zhang²,
Daniel Harabor², Stephen F. Smith¹, Jiaoyang Li¹

Abstract—We present Scalable Multi-Agent Realistic Testbed (SMART), a realistic and efficient software tool for evaluating Multi-Agent Path Finding (MAPF) algorithms. MAPF focuses on planning collision-free paths for a group of agents. While state-of-the-art MAPF algorithms can plan paths for hundreds of robots in seconds, they often rely on simplified robot models, making their real-world performance unclear. Researchers typically lack access to hundreds of physical robots in laboratory settings to evaluate the algorithms. Meanwhile, industrial professionals who lack expertise in MAPF require an easy-to-use simulator to efficiently test and understand the performance of MAPF algorithms in their specific settings. SMART fills this gap with several advantages: (1) SMART uses physics-engine-based simulators to create realistic simulation environments, accounting for complex real-world factors such as robot kinodynamics and execution uncertainties, (2) SMART uses an execution monitor framework based on the Action Dependency Graph, facilitating seamless integration with various MAPF algorithms and robot models, and (3) SMART scales to thousands of robots. The code is publicly available at <https://github.com/smart-mapf/smart>.

Index Terms—Multi-Agent Path Finding, Multi-Robot System, Realistic Simulation.

I. INTRODUCTION

The Multi-Agent Path Finding (MAPF) problem [1] focuses on planning collision-free paths for a large group of robots within a known environment. This problem finds various real-world applications [2]–[4], with warehouse automation being a prominent example, where hundreds of robots must be coordinated to perform daily operations. In recent years, MAPF has grown into a rapidly expanding research area [5], [6]. State-of-the-art MAPF algorithms can plan paths for hundreds of robots within seconds [7]–[9]. However, these algorithms make several simplifying assumptions. First, they rely on simplified robot models that ignore kinodynamic constraints while planning the robots’ paths. Second, they assume that robots can execute these paths perfectly, without accounting for uncertainties introduced by real-world factors. Therefore, while researchers have shown that MAPF algorithms have a wide range of applications, their performance in more realistic settings is unclear.

MAPF researchers in both academia and industry require an efficient, realistic, and scalable software tool to evaluate MAPF algorithms in realistic settings. In academia, deploying

¹J. Yan, Z. Li, W. Kang, Y. Zhang, S. Smith, and J. Li are with Robotics Institute, Carnegie Mellon University, Pittsburgh, PA 15213, USA (email: jingtianyan, zhifeili, williamkang, yulunzhang@cmu.edu, ssmith@andrew.cmu.edu, jiaoyangli@cmu.edu).

²K. Zheng, Z. Chen, Y. Zhang, and D. Harabor are with Monash University, Clayton, VIC 3800, Australia. (email: kevin.zheng, zhe.chen, yue.zhang, daniel.harabor@monash.edu).

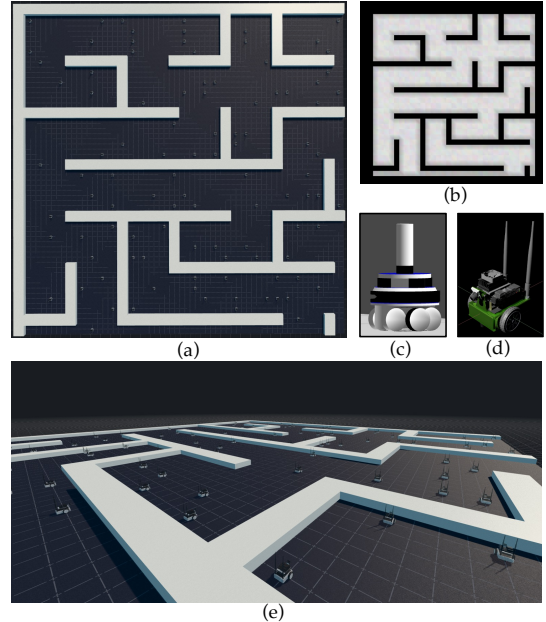


Fig. 1: (a) A simulation environment in SMART. (b) The original 2-D grid map from the MovingAI benchmark. (c, d) Robot models used in the environment. (e) A 3D view of the environment.

hundreds of physical robots in a large environment to evaluate MAPF algorithms is impractical. Meanwhile, developing software that can evaluate large groups of robots is a non-trivial task for MAPF researchers. Researchers must create high-fidelity simulation environments and robot models to capture realistic factors, as well as develop essential software components such as controllers and execution frameworks to execute their plans. Moreover, since many researchers come from the AI community, learning such simulation tools can be time-consuming and require significant effort. While some software tools [10], [11] have been developed to evaluate MAPF algorithms in realistic settings, they do not scale to hundreds of robots and require significant engineering efforts to integrate new MAPF algorithms and maps. In addition, industrial professionals possess realistic simulators for their applications of interest. However, they may not have the resources and expertise to implement state-of-the-art MAPF algorithms in their simulators. By having a realistic simulator that can easily interface with existing implementations of MAPF algorithms, industrial professionals can more easily understand and select a MAPF algorithm that fits their demands.

In this paper, we present SMART, a Scalable Multi-Agent Realistic Testbed, a software tool used to evaluate MAPF

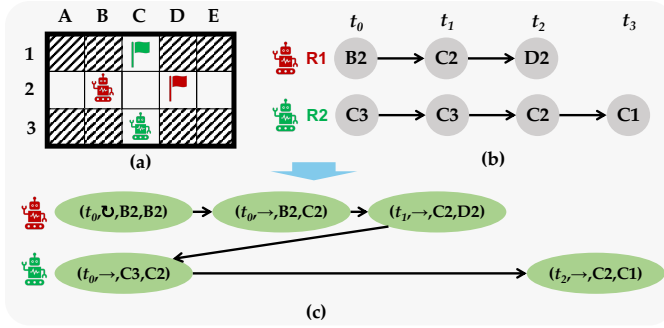


Fig. 2: (a) MAPF problem. (b) Associated MAPF plan. (c) ADG from the MAPF plan. Green ovals are actions, with the first element as the reference time from the plan, the second as the action type, and the last two as start and goal locations. Horizontal edges are Type-1, and vertical edges are Type-2. All robots initially face north.

algorithms in realistic scenarios. SMART comprises three main components: (1) physics-engine-based simulators, (2) an execution monitoring (EM) server, and (3) robot-specific executors. The simulator generates realistic simulation environments based on user-defined configurations. Fig. 1 shows an example environment in SMART created from a 2-D grid map from the MovingAI benchmark [1]. The EM server parses the user-provided MAPF paths, tracks the execution progress, and communicates with the executors. It leverages the Action Dependency Graph (ADG) [3], a MAPF execution framework, to ensure robust execution of the paths generated using various simplified robot models. Each robot is assigned an individual executor that receives and executes actions from the server. SMART incorporates key real-world factors, including robot kinodynamics, collision dynamics, communication delays, execution imperfections, and temporal uncertainty during execution.

Our contributions in this paper are as follows: 1. We present SMART, an open-source software tool for evaluating MAPF algorithms in realistic scenarios. SMART directly accepts MAPF plans and problem instances from existing benchmarks. 2. We integrate SMART with two simulators, ARGoS3 and Isaac Sim, and robot models and empirically evaluate its scalability and replicability. SMART can scale to thousands of robots while maintaining consistent and reproducible results, while prior tools fail to handle a hundred robots. 3. We develop an online interface with interactive visualization, allowing users to easily monitor execution progress and access detailed statistical data during simulation. 4. We validate SMART on real-world mobile robots, demonstrating its robustness and effectiveness in physical environments.

II. BACKGROUND

In this section, we first introduce the MAPF problem and related work. Next, we discuss existing execution frameworks for executing MAPF plans. Finally, we review benchmarks used to evaluate MAPF algorithms.

A. MAPF Problem and MAPF Plan

A MAPF instance [1] consists of an undirected graph $\mathcal{G}_M = (\mathcal{V}_M, \mathcal{E}_M)$ constructed from a 2-D grid map and a set of I

robots $\mathcal{R} = \{r_1, \dots, r_I\}$ with their corresponding start and goal locations. Given a MAPF instance, a MAPF algorithm aims at finding a MAPF plan, consisting of collision-free paths for all robots from their start to goal locations. Standard MAPF uses a simplified robot model by discretizing the time into timesteps and assuming that, at each timestep, every robot either moves to an adjacent vertex or stays at its current vertex. Two robots collide if they are at the same vertex or swap vertices at the same timestep. An example MAPF instance and plan on a 2-D grid graph are shown in Fig. 2 (a) and (b), respectively. The objective of MAPF is to minimize the sum-of-cost, defined as the sum of travel time.

Prior research has proposed many MAPF algorithms, most of which are developed based on 2-D grid maps. Some methods focus on finding solutions with optimal or bounded-suboptimal guarantees [12], [13], while others focus on scalability, solving MAPF problems involving thousands of robots [14], [15]. Anytime algorithms quickly find an initial solution and then iteratively refine it as time progresses, balancing solution quality with computational efficiency [16], [17]. Additionally, some methods incorporate complex real-world factors, such as kinodynamics and unexpected delays, into the planning process [18]–[21]. They usually employ a two-level planner, where the high level employs MAPF-based methods to resolve collisions among agents, while the low level plans for each agent, consider real-world factors.

B. Executing MAPF Plans

Given a MAPF plan, robots can remain collision-free if they strictly follow it spatially and temporally. While existing path-tracking techniques allow for reasonable spatial accuracy, precise temporal adherence is more challenging [22], especially since MAPF plans are typically generated using imperfect robot models. Thus, we need techniques to execute MAPF plans safely given the uncertainty in execution time. One naive way is synchronized execution, where agents need to wait for all robots to finish their current action before starting the next. This ensures strict compliance with the MAPF plan but significantly reduces efficiency. Alternatively, one can replan whenever a robot is delayed, but this is computationally heavy and thus does not scale well. Therefore, executing MAPF plans using an execution framework is preferred [22]. The state-of-the-art execution framework is Action Dependency Graph (ADG) [3], which enforces passing orders defined by MAPF plans while accounting for delays. ADG can execute plans generated by MAPF planners of various robot models [23].

An ADG, as shown in Fig. 2 (c), is a directed graph $\mathcal{G} = (\mathcal{V}, \mathcal{E}_1, \mathcal{E}_2)$ that encodes dependencies between actions from a MAPF plan. The vertex set $\mathcal{V} = \{v_i^k : k \in [1, n^i], r_i \in \mathcal{R}\}$ represents all actions performed by each robot r_i , where each vertex v_i^k corresponds to the k -th action of r_i , and n^i is its number of actions. The edge set \mathcal{E}_1 includes Type-1 edges, which enforce the sequential execution of actions by each robot. For a robot r_i , a Type-1 edge (v_i^k, v_i^{k+1}) ensures that action v_i^k is completed before action v_i^{k+1} starts. The edge set \mathcal{E}_2 includes Type-2 edges, which enforce the inter-robot passing order at shared vertices. For any two vertices v_i^k and v_j^s

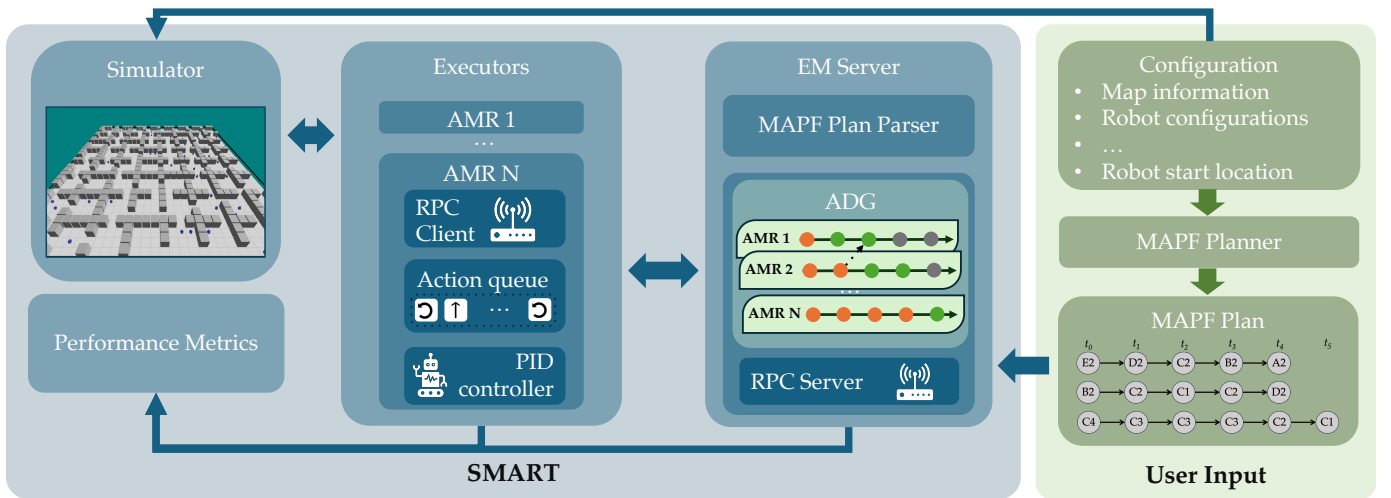


Fig. 3: System overview of SMART.

from r_i and r_j , a Type-2 edge (v_i^k, v_j^s) ensures that v_i^k must be completed before v_j^s can start. During execution, each action is performed according to these dependencies. The detailed execution procedure is described in Section III-B.

C. Evaluating MAPF Plans

To evaluate MAPF algorithms, researchers typically generate a plan for a given MAPF instance and then execute it. While many MAPF benchmarks with 2-D-grid maps are proposed [1], [24]–[26], most prior MAPF works are evaluated on them using simplified robot models that assume no delays and discretized time and space. Some benchmarks have attempted to include realistic elements such as acceleration and rotation [27], [28]. However, their model is still far from realistic, and typically requires the same robot models for both planning and execution phases.

Given the difficulty of modeling all real-world factors analytically, physics-engine-based simulators offer a promising approach for more accurate evaluation. MRP-Bench [10] leverages a high-fidelity, physics-based simulator Gazebo [29] to simulate multi-robot systems. It integrates low-level controllers to account for robots’ kinodynamic constraints and potential delays. REMROC [11] also uses Gazebo to realistically evaluate MAPF plans, with a particular focus on human-shared environments. However, these existing tools have two main limitations. First, they often require significant engineering effort to integrate user-defined maps and MAPF planners, limiting their flexibility for different scenarios. In particular, they lack a general execution framework, making it difficult to directly evaluate MAPF planners using different robot models. Second, they have limited scalability: the largest number of robots tested in previous work is less than 100 agents. Most of these works rely on Gazebo, whose high computational overhead, resulting from modeling many factors not relevant to MAPF, significantly constrains scalability. MRP-Bench, for example, does not scale to more than 10 robots.

III. SMART ARCHITECTURE

Fig. 3 shows an overview of SMART. It comprises three main modules: a simulator, an execution monitoring (EM) server, and executors. All modules are implemented in C++. The simulator generates simulation environments based on the user-provided configurations. The EM server parses the MAPF plan and monitors the execution status of each action throughout the simulation. When an action is ready for execution, the server sends the action to the corresponding robot via the network. The executor of each robot receives actions from the server, executes them using a controller, and synchronizes the execution status with the server accordingly.

A. Simulator

Given a user-provided configuration, the simulator creates realistic simulation environments. The configuration specifies obstacle locations and shapes, robot start locations, and detailed robot configurations (e.g., the robot model, as well as its velocity and acceleration limits). To support the widely used MovingAI benchmark [1], SMART can convert its 2-D grid maps and corresponding MAPF instances into the configuration required by the simulator. During execution, the simulator uses a physics engine to update the states of the robots and environment, including their poses, dynamics, sensors, and actuators, based on the received control commands from the executors. The executors can query the simulator for real-time robot information, such as their current pose. To accommodate diverse user requirements, SMART supports two simulation platforms: ARGoS3 [30] and Isaac Sim [31].

1) *ARGoS3*: ARGoS3 is a multi-robot simulator with excellent scalability, advanced physics engines, and support for custom robot and environment models, making it suitable for our tasks. While users can specify any robot model, we use the foot-bot (shown in Fig. 1 (c)), a differential-drive robot, in our experiments. It closely resembles robots used in real-world warehouses and can move forward and rotate in place.

2) *Isaac Sim*: Isaac Sim is a high-fidelity robotics simulator developed by NVIDIA, featuring GPU-accelerated physics,

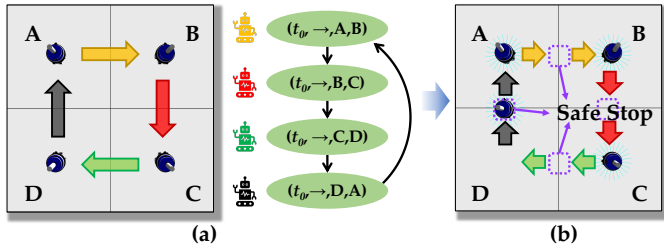


Fig. 4: (a) Cycle in the ADG causing all robots to be stalled. (b) Adding safe stops between vertices to make the ADG acyclic.

photorealistic rendering, and seamless integration with ROS. It is well-suited for sim-to-real transfer and physically grounded perception and control tasks. We use the JetBot robot (shown in Fig. 1 (d)), a differential-drive robot commonly used in research and education.

B. Execution Monitoring (EM) Server

The EM server parses the MAPF plan and encodes its passing order into an ADG. It then manages the execution of the MAPF plan and communicates with the executors.

Server Initialization: During the initialization, we use the MAPF plan parser to construct an ADG. We define a standardized format to store the MAPF plan as a sequence of timed locations for each robot r_i , i.e., $((x_i^0, y_i^0, t_i^0), \dots, (x_i^T, y_i^T, t_i^T))$. The parser can take as input any valid MAPF plans of this format, regardless of the MAPF planners that generate the plans. This allows SMART to work with plans using varying simplified robot models. The parser first converts the path of each robot into a sequence of actions. Specifically, the parser infers the orientation of a robot by comparing consecutive vertices along its path and adds a rotation action when needed. The ADG is constructed based on the sequence of actions. ADG requires the MAPF plan to be circle-conflict free, ensuring that robots do not collide even if delayed by one timestep [3]. However, ensuring this is not standard in most MAPF models. As a result, if we directly build an ADG based on a plan with circle conflict, we may create deadlocks, such as the one illustrated in Fig. 4 (a). While these robots are planned to rotate simultaneously in a cycle, with ADG, they will end up waiting indefinitely for others to complete their next actions. To accommodate a broader range of planners, motivated by [32], we add an extra vertex between consecutive vertices in SMART as shown in Fig. 4 (b), making the ADG compatible with these MAPF models.

Execution Managing: During execution, an execution monitor framework manages the progress of execution and communicates with robot executors. This framework follows the method described in ADG [3] to track and manage execution. Each vertex in the ADG represents an action and can have one of three statuses: *staged*, *enqueued*, or *finished*. At first, all vertices are *staged*. A vertex transitions to *enqueued* if (1) it has no preceding vertices, or (2) its preceding vertex connected by a Type-1 edge is *enqueued* or *finished*, and all its preceding vertices connected by Type-2 edges are *finished*. Actions associated with *enqueued* vertices are then sent to the executors for execution. A vertex is marked as *finished*

when the executor confirms the completion of its associated action with the server. Communication with robot executors is managed by an RPC server built with `rpclib`¹.

C. Executor

Each robot is launched with an individual executor. As shown in Fig. 3, each executor consists of an RPC client, an action queue, and a controller. The RPC client establishes communication with the server, receiving *enqueued* actions and sending confirmation for *finished* actions. The action queue keeps track of the *enqueued* actions, which are executed in a first-in-first-out manner. A Proportional Integral Derivative (PID) controller is used to execute these actions by sending control commands to the simulator. Once an action is finished, a confirmation message is sent to the server. To allow robots to operate at higher speeds, consecutive actions of the same type are merged into one action in the queue. For example, if a robot receives three consecutive forward movement actions, the executor merges them into a single longer forward action, reducing unnecessary stop-and-go behavior.

D. Performance Metrics

SMART provides several built-in performance metrics, including (1) *Average execution time (AET)*: The sum of the simulation times required by all robots to complete their assigned paths, divided by the number of robots, (2) *Maximum execution time*: The longest simulation time taken by any single robot to complete its path, and (3) *Robot state over time*: The state of each robot at different times, where the state includes the size of its action queue, its current position, and its current wheel velocity. Additionally, the open-source nature of our code allows researchers to easily derive custom metrics from SMART as needed. SMART also provides visualization for the MAPF plan executions, allowing researchers to better understand the behaviors of the robots.

IV. USING SMART

Users can evaluate their solutions using SMART in two ways: by uploading their MAPF problem and solution through a web interface or by deploying SMART locally.

SMART as a Service: SMART, with ARGOS3 and the 3D visualizer, is directly available as software-as-a-service². Specifically, we provide an intuitive web app for running and inspecting MAPF simulations. Complete with a beautiful 3D-visualizer built with React and Three.js, it allows researchers to instantly understand how algorithms perform with physical robots (Fig. 5). Users configure the environment by specifying a map and scenario file in the MovingAI Benchmark format. Within the online interface, after users upload the files and select the desired kinodynamic settings for the robots, and initiate the simulation with a single click. After starting the simulation, they can control the simulation time step and adjust the playback speed. Users may select robots to view complete paths, execution status, and Type-2 edges between robots.

¹Available at <http://rpclib.net>.

²The link will be made available here upon acceptance.

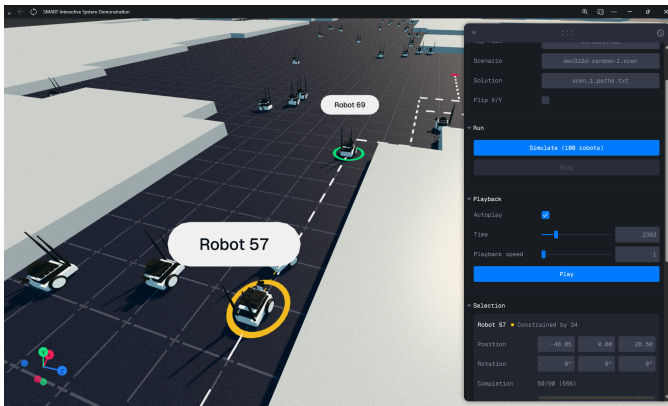


Fig. 5: The SMART web interface visualizing a multi-robot simulation on a grid map. In the viewport, users interact with individual robots to inspect paths and inter-robot constraints. On the side panel, users can configure the environment, control playback, and see execution details.

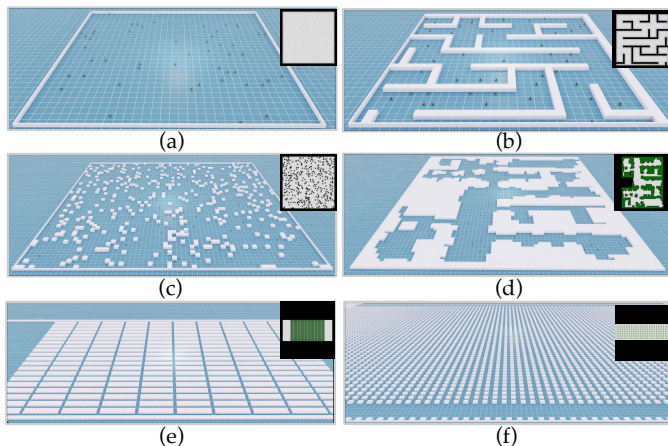


Fig. 6: Simulation environments. (a) empty (b) maze (c) random (d) game (e) warehouse (f) sortation-center.

Installing SMART Locally: Since SMART provides flexible interfaces for customization, researchers may choose to compile it locally for advanced use cases, such as running it in headless mode, integrating it into custom pipelines, or interfacing with real robots. As an open-source tool, SMART includes documentation and examples to support these advanced configurations.

V. SYSTEM EVALUATION

We test SMART on two machines. All experiments are conducted on machine (1), a high-performance server with a 64-core AMD 7980X processor, 256 GB of memory, and RTX 3090Ti GPU. In Section V-C, we additionally test SMART on machine (2), a low-end laptop with a 4-core Intel i7-6700HQ processor and 16 GB of memory, to demonstrate SMART’s performance on resource-constrained hardware. Both machines are equipped with Ubuntu 20.04.

As shown in Fig. 6, we evaluate SMART on six environments converted from: *empty* (*empty-32-32*, size: 32×32), *maze* (*maze-32-32-4*, size: 32×32), *random* (*random-64-64-10*, size: 64×64), *game* (*den312d*, size: 65×81), *warehouse*

(*warehouse-10-20-10-2-1*, size: 161×63) from the MovingAI benchmark [1] and *sortation-center* (size: 500×140) from the League of Robot Runner MAPF competition [28].

In all experiments, the simulation update period is set to 0.1 simulation seconds for both simulators. A simulation update refers to the periodic recalculation of the status of robots and the environment based on the input commands. In ARGoS3, each grid cell represents 1 meter. Each foot-bot robot is subject to a speed limit of $[0, 5]$ m/s, an acceleration limit of $[-0.4, 0.4]$ m/s², and an angular velocity limit of 30° /s. In Isaac Sim, each grid cell represents 0.5 meters. Each JetBot is constrained to a speed limit of $[0, 2.5]$ m/s, an acceleration limit of $[-0.2, 0.2]$ m/s², and the same angular velocity limit of 30° /s.

We evaluated our system using MAPF plans generated by three different methods: CBS [12], PBS [7], and MAPF-LNS2 [9]. These plans were created using four different robot models: the standard MAPF model [1], the k -robust delay model [19], MAPF with rotation [33], and MAPF with kinodynamics [21]. Across all combinations, our system achieved a 100% execution success rate. In the remainder of this section, we present results based on MAPF plans generated by MAPF-LNS2, as it demonstrated the highest scalability among the algorithms evaluated.

A. Scalability and Runtime Performance

This section evaluates the scalability and runtime performance of SMART by analyzing its simulation speed, which is defined as the ratio of the simulation time to the real-world time. A higher simulation speed means that more simulation updates can be finished within the same unit of time, indicating better scalability. For example, if the simulation speed is 10, the simulation world runs 10 times faster than in real time. MAPF plans are generated using MAPF-LNS2³ [9] with a progressively increasing number of robots and a time limit of 60 seconds. For each map, we randomly select 5 scenarios from the MovingAI Benchmark to generate plans, which are then executed in SMART without visualization. In ARGoS3, the maximum number of robots tested corresponds to the limit imposed by the MAPF instances from the MovingAI Benchmark for all maps except *sortation-center*, which is set to 2,000 robots. In contrast, for Isaac Sim, the upper bound on the number of robots is determined by the point at which the simulation speed drops below real-time (i.e., simulation speed < 1).

As shown in Fig. 7, SMART supports simulations with up to 2,000 robots. The more robots and the larger the map, the smaller the simulation speed. Nevertheless, for ARGoS3, SMART maintains a simulation speed of around 10.0 with 1,000 robots in *warehouse*. Even in the larger *sortation-center*, the simulation speed is consistently greater than 1.0. In contrast, Isaac Sim provides the capability to model more complex real-world factors while also producing photorealistic visualizations, but it is significantly less scalable, particularly in large environments. It is therefore more suitable for experiments with a smaller number of agents.

³Code at <https://github.com/Jiaoyang-Li/MAPF-LNS2>

Simulator	Robots (#)	average execution time	maximum execution time
ARGoS3	10	123.33 \pm 0.00	373.6 \pm 0.00
	50	182.84 \pm 0.01	433.30 \pm 0.00
	100	263.36 \pm 0.01	469.80 \pm 0.00
	200	269.79 \pm 0.02	675.50 \pm 0.00
	400	385.76 \pm 0.02	737.60 \pm 0.42
	600	462.87 \pm 0.07	843.70 \pm 0.71
	1000	612.04 \pm 0.07	1389.43 \pm 0.83
Isaac Sim	10	122.47 \pm 0.00	369.47 \pm 0.00
	50	183.71 \pm 0.07	435.46 \pm 1.36

TABLE I: Replicability using different numbers of robots.

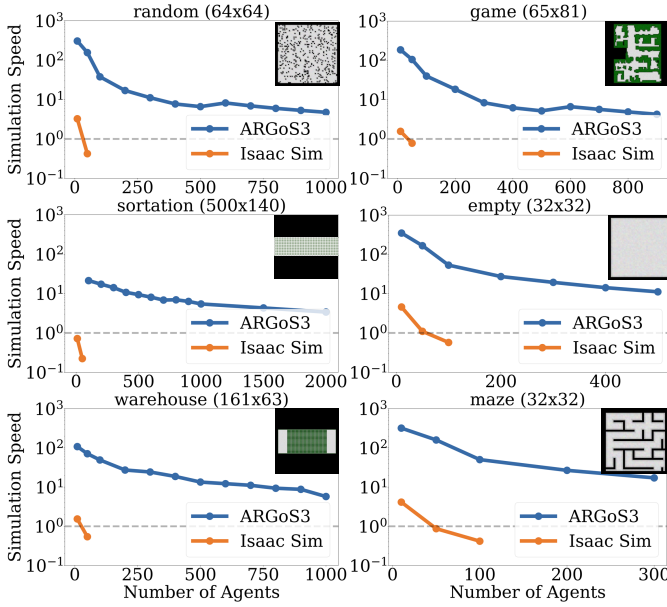


Fig. 7: Simulation speed on all environments.

B. Replicability

We evaluate the consistency of SMART by examining whether the same MAPF plans yield the same outcomes across multiple runs. Due to the realistic setting we used, uncertainty may arise from factors such as network communication delays or controller variability. Using the same *warehouse* map and MAPF plans as in the previous section, we execute SMART 10 times for each MAPF plan. For each run, we record both the average and the maximum execution time. As shown in Table I, SMART demonstrates strong replicability across runs, with minor execution time variations. While these variations increase slightly with more robots, they remain minimal even for up to a thousand robots.

C. CPU and Memory Usage

We evaluate the CPU and memory usage of SMART on both machines (1) and (2). We use machine (2) to demonstrate that SMART can run on resource-constrained machines. To evaluate usage, we generate MAPF plans with MAPF-LNS2 and run SMART on the *warehouse* map with different numbers of robots, each with 5 random MAPF instances selected from the MAPF benchmark [1]. All simulations are

	Sim	Robots (#)	CPU Usage (%)	Memory Usage (GB)	Simulation Speed
Machine (1)	ARGoS3	10	2.99 \pm 0.10	0.03 \pm 0.02	107.93 \pm 1.80
		50	8.03 \pm 0.08	0.07 \pm 0.00	62.35 \pm 2.33
		100	16.48 \pm 0.58	0.19 \pm 0.26	33.49 \pm 0.15
		500	22.86 \pm 1.59	0.24 \pm 0.01	13.21 \pm 0.13
		1000	46.02 \pm 0.98	0.65 \pm 0.03	7.37 \pm 0.04
	Isaac Sim	10	25.53 \pm 4.29	10.16 \pm 0.82	1.35 \pm 0.01
		50	27.18 \pm 2.97	10.94 \pm 7.25	0.54 \pm 0.00
		100	N/A	N/A	N/A
		500	N/A	N/A	N/A
		1000	N/A	N/A	N/A
Machine (2)	ARGoS3	10	18.54 \pm 3.88	0.01 \pm 0.01	37.67 \pm 1.02
		50	20.20 \pm 0.91	0.05 \pm 0.03	21.42 \pm 0.35
		100	27.96 \pm 0.39	0.04 \pm 0.00	14.37 \pm 0.10
		500	68.74 \pm 17.24	0.22 \pm 0.01	3.89 \pm 0.02
		1000	59.64 \pm 0.32	0.63 \pm 0.02	1.95 \pm 0.01

TABLE II: Comparison of CPU usage, memory consumption, and simulation speed for ARGoS3 and Isaac Sim across two machines and various robot counts. Since Isaac Sim only supports recent GPUs with ray tracing capabilities, we conducted experiments with Isaac Sim only on Machine (1).

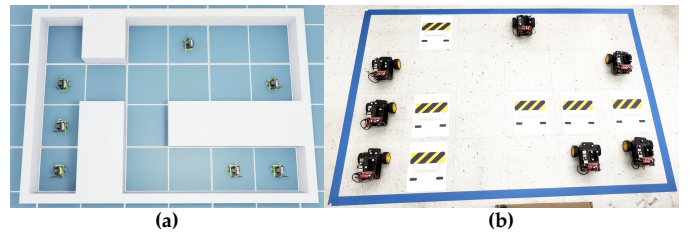


Fig. 8: (a) Experimental setup in Isaac Sim. (b) Experimental setup with real robots.

parallelized on all CPU cores on both machines. We record the peak CPU and memory usage while running the simulation and compute the average of all instances for each number of robots. Table II shows the results. When using ARGoS3 as the simulator, we observe that SMART has reasonable CPU usage and low memory usage on both machines, making it possible to run on low-spec personal laptops. The simulation speed in machine (2) is slower than in machine (1) due to an inferior processor. In contrast, simulations with Isaac Sim result in significantly higher CPU and memory usage, indicating that Isaac Sim is better suited for scenarios with fewer agents but more powerful hardware.

D. Evaluation in Real World

Finally, we demonstrate the execution of SMART on real-world mobile robots. Specifically, we deploy SMART on a team of seven JetBot differential-drive robots operating in a structured indoor environment, as illustrated in Fig. 8. The environment is configured as a 4 \times 6 grid, with each cell measuring 0.3 \times 0.3 meters, and both obstacles and boundaries are physically defined. A Vicron motion capture system provides accurate real-time localization for the robots.

Given a set of start and goal locations, MAPF-LNS2 is used on a central server to generate a MAPF plan. SMART then processes this plan and transmits control commands to each robot via a wireless network, with a control frequency of 40 Hz. Each JetBot follows its assigned commands accordingly.

As shown in the accompanying multimedia material, SMART robustly executes the MAPF plan on physical robots, highlighting the practical feasibility and reliability of our planning framework in real-world scenarios. Across 10 trials, SMART achieved a 100% success rate, with an average execution time of 48.48 ± 8.79 seconds and a maximum execution time of 73.83 ± 9.81 seconds. For reference, in Isaac Sim, the average execution time is 45.66 ± 0.01 seconds, and the maximum execution time is 70.97 ± 0.00 seconds.

VI. CONCLUSION

We introduce SMART, a scalable testbed for evaluating MAPF algorithms under realistic settings. SMART bridges the gap between methods that use simplified MAPF models and their real-world deployments. SMART is compatible with existing 2-D grid-based benchmarks, making it straightforward for researchers to evaluate their methods in more realistic environments. We integrate SMART with two simulators, ARGoS3 and Isaac Sim. Our experiments show that SMART can handle thousands of robots while maintaining high simulation speeds when using ARGoS3. Future work includes extending the framework to address lifelong MAPF scenarios and integrating it with other execution frameworks [34]–[36].

REFERENCES

- [1] R. Stern, N. R. Sturtevant, A. Felner, S. Koenig, H. Ma, T. T. Walker, J. Li, D. Atzmon, L. Cohen, T. K. S. Kumar, E. Boyarski, and R. Barták, “Multi-agent pathfinding: Definitions, variants, and benchmarks,” in *Proceedings of the International Symposium on Combinatorial Search*, 2019, pp. 151–159.
- [2] H. Ma, J. Yang, L. Cohen, T. Kumar, and S. Koenig, “Feasibility study: Moving non-homogeneous teams in congested video game environments,” in *Proceedings of the AAAI Conference on Artificial Intelligence and Interactive Digital Entertainment*, vol. 13, no. 1, 2017, pp. 270–272.
- [3] W. Höning, S. Kiesel, A. Tinka, J. W. Durham, and N. Ayanian, “Persistent and robust execution of MAPF schedules in warehouses,” *IEEE Robotics and Automation Letters*, vol. 4, no. 2, pp. 1125–1131, 2019.
- [4] F. Ho, A. Gonçalves, B. Rigault, R. Gerales, A. Chicharo, M. Cavazza, and H. Prendinger, “Multi-agent path finding in unmanned aircraft system traffic management with scheduling and speed variation,” *IEEE Intelligent Transportation Systems Magazine*, vol. 14, no. 5, pp. 8–21, 2022.
- [5] H. Ma, “Graph-based multi-robot path finding and planning,” *Current Robotics Reports*, vol. 3, no. 3, pp. 77–84, 2022.
- [6] S. Wang, H. Xu, Y. Zhang, J. Lin, C. Lu, X. Wang, and W. Li, “Where paths collide: A comprehensive survey of classic and learning-based multi-agent pathfinding,” *arXiv preprint*, vol. arXiv:2505.19219, 2025.
- [7] H. Ma, D. Harabor, P. J. Stuckey, J. Li, and S. Koenig, “Searching with consistent prioritization for multi-agent path finding,” in *Proceedings of the AAAI Conference on Artificial Intelligence*, vol. 33, 2019, pp. 7643–7650.
- [8] H. Zhang, J. Li, P. Surynek, T. K. S. Kumar, and S. Koenig, “Multi-agent path finding with mutex propagation,” *Artificial Intelligence*, vol. 311, p. 1034766, 2022.
- [9] J. Li, Z. Chen, D. Harabor, P. J. Stuckey, and S. Koenig, “MAPF-LNS2: Fast repairing for multi-agent path finding via large neighborhood search,” in *Proceedings of the AAAI Conference on Artificial Intelligence*, vol. 36, 2022, pp. 10256–10265.
- [10] S. Schaefer, L. Palmieri, L. Heuer, R. Dillmann, S. Koenig, and A. Kleiner, “A benchmark for multi-robot planning in realistic, complex and cluttered environments,” in *Proceedings of the IEEE International Conference on Robotics and Automation*, 2023, pp. 9231–9237.
- [11] L. Heuer, L. Palmieri, A. Mannucci, S. Koenig, and M. Magnusson, “Benchmarking multi-robot coordination in realistic, unstructured human-shared environments,” in *Proceedings of the IEEE International Conference on Robotics and Automation*, 2024, pp. 14541–14547.
- [12] G. Sharon, R. Stern, A. Felner, and N. R. Sturtevant, “Conflict-based search for optimal multi-agent pathfinding,” *Artificial Intelligence*, vol. 219, pp. 40–66, 2015.
- [13] J. Li, W. Ruml, and S. Koenig, “EECBS: A bounded-suboptimal search for multi-agent path finding,” in *Proceedings of the AAAI Conference on Artificial Intelligence*, vol. 35, 2021, pp. 12353–12362.
- [14] K. Okumura, M. Machida, X. Défago, and Y. Tamura, “Priority inheritance with backtracking for iterative multi-agent path finding,” *Artificial Intelligence*, vol. 310, p. 103752, 2022.
- [15] K. Okumura, “LaCAM: Search-based algorithm for quick multi-agent pathfinding,” in *Proceedings of the AAAI Conference on Artificial Intelligence*, vol. 37, no. 10, 2023, pp. 11655–11662.
- [16] J. Li, Z. Chen, D. Harabor, P. J. Stuckey, and S. Koenig, “Anytime multi-agent path finding via large neighborhood search,” in *Proceedings of the International Joint Conference on Artificial Intelligence*, 2021, pp. 4127–4135.
- [17] T. Huang, J. Li, S. Koenig, and B. Dilkina, “Anytime multi-agent path finding via machine learning-guided large neighborhood search,” in *Proceedings of the AAAI Conference on Artificial Intelligence*, 2022, pp. 9368–9376.
- [18] L. Cohen, T. Uras, T. K. S. Kumar, and S. Koenig, “Optimal and bounded-suboptimal multi-agent motion planning,” in *Proceedings of the International Symposium on Combinatorial Search*, vol. 10, 2019, pp. 44–51.
- [19] D. Atzmon, R. Stern, A. Felner, G. Wagner, R. Barták, and N.-F. Zhou, “Robust multi-agent path finding and executing,” *Journal of Artificial Intelligence Research*, vol. 67, pp. 549–579, 2020.
- [20] J. Yan and J. Li, “Multi-agent motion planning with bézier curve optimization under kinodynamic constraints,” *IEEE Robotics and Automation Letters*, vol. 9, no. 3, pp. 3021–3028, 2024.
- [21] —, “Multi-agent motion planning for differential drive robots through stationary state search,” in *Proceedings of the AAAI Conference on Artificial Intelligence*, vol. 39, no. 22, 2025, pp. 23360–23368.
- [22] M. Čáp, J. Gregoire, and E. Frazzoli, “Provably safe and deadlock-free execution of multi-robot plans under delaying disturbances,” in *Proceedings of the IEEE International Conference on Intelligent Robots and Systems*, 2016, pp. 5113–5118.
- [23] S. Varambally, J. Li, and S. Koenig, “Which MAPF model works best for automated warehousing?” in *Proceedings of the International Symposium on Combinatorial Search*, vol. 15, 2022, pp. 190–198.
- [24] M. Gebser, P. Obermeier, T. Otto, T. Schaub, O. Sabuncu, V. Nguyen, and T. C. Son, “Experimenting with robotic intra-logistics domains,” *Theory and Practice of Logic Programming*, vol. 18, no. 3-4, pp. 502–519, 2018.
- [25] N. R. Sturtevant, “Benchmarks for grid-based pathfinding,” *IEEE Transactions on Computational Intelligence and AI in Games*, vol. 4, no. 2, pp. 144–148, 2012.
- [26] C. Qian, Y. Zhang, V. Bhatt, M. C. Fontaine, S. Nikolaidis, and J. Li, “A quality diversity method to automatically generate multi-agent path finding benchmark maps,” *arXiv preprint*, vol. arXiv:2409.06888, 2024.
- [27] S. Mohanty, E. Nygren, F. Laurent, M. Schneider, C. Scheller, N. Bhattacharya, J. Watson, A. Egli, C. Eichenberger, C. Baumberger, G. Vienken, I. Sturm, G. Sartoretti, and G. Spigler, “Flatland-RL: Multi-agent reinforcement learning on trains,” *arXiv preprint*, vol. arXiv:2012.05893, 2020.
- [28] S.-H. Chan, Z. Chen, T. Guo, H. Zhang, Y. Zhang, D. Harabor, S. Koenig, C. Wu, and J. Yu, “The League of Robot Runners Competition: Goals, Designs, and Implementation,” in *Proceedings of the 34th International Conference on Automated Planning and Scheduling – System Demonstrations Track*, 2024.
- [29] N. Koenig and A. Howard, “Design and use paradigms for gazebo, an open-source multi-robot simulator,” in *Proceedings of the IEEE International Conference on Intelligent Robots and Systems*, vol. 3, 2004, pp. 2149–2154.
- [30] C. Pinciroli, V. Trianni, R. O’Grady, G. Pini, A. Brutschy, M. Brambilla, N. Mathews, E. Ferrante, G. Di Caro, F. Ducatelle *et al.*, “ARGoS: A modular, parallel, multi-engine simulator for multi-robot systems,” *Swarm intelligence*, vol. 6, pp. 271–295, 2012.
- [31] NVIDIA, “Isaac Sim,” <https://developer.nvidia.com/isaac-sim>, 2023, accessed: 2025-07-10.
- [32] W. Höning, T. K. S. Kumar, L. Cohen, H. Ma, H. Xu, N. Ayanian, and S. Koenig, “Multi-agent path finding with kinematic constraints,” in *Proceedings of the International Conference on Automated Planning and Scheduling*, vol. 26, 2016, pp. 477–485.
- [33] Y. Zhang, D. Harabor, P. Le Bodic, and P. J. Stuckey, “Efficient multi agent path finding with turn actions,” in *Proceedings of the International Symposium on Combinatorial Search*, vol. 16, no. 1, 2023, pp. 119–127.

- [34] A. Coskun and J. M. O’Kane, “Online plan repair in multi-robot coordination with disturbances,” in *Proceedings of the IEEE International Conference on Robotics and Automation*, 2019, pp. 3333–3339.
- [35] A. Berndt, N. Van Duijkeren, L. Palmieri, A. Kleiner, and T. Keviczky, “Receding horizon re-ordering of multi-agent execution schedules,” *IEEE Transactions on Robotics*, vol. 40, pp. 1356–1372, 2024.
- [36] Y. Feng, A. Paul, Z. Chen, and J. Li, “A real-time rescheduling algorithm for multi-robot plan execution,” in *Proceedings of the International Conference on Automated Planning and Scheduling*, vol. 34, 2024, pp. 201–209.